MODEL OF PLASMA IMMERSION ION IMPLANTATION

by

M. A. Lieberman

Memorandum No. UCB/ERL M89/30

20 March 1989

ELECTRONICS RESEARCH LABORATORY

College of Engineering
University of California, Berkeley
94720

TITLE PAGE

MODEL OF PLASMA IMMERSION ION IMPLANTATION

M. A. LIEBERMAN

Department of Electrical Engineering and Computer Sciences
and the Electronics Research Laboratory
University of California, Berkeley, CA 94720

ABSTRACT

In plasma immersion ion implantation, a target is immersed in a plasma and a series of negative high voltage pulses are applied to implant plasma ions into the target. We develop an approximate analytical model to determine the time-varying implantation current, the total dose, and the energy distribution of the implanted ions.

I. INTRODUCTION

In ion implantation, energetic ions are injected into the surface of a solid material with the result that the atomic composition and structure of the near-surface region is changed. The process is routine in semiconductor device fabrication. Metallurgical implantation is an emerging technology; in this application, new surface alloys are created with improved resistance to wear, corrosion, and fatigue.

Conventional implantation is carried out in a high vacuum environment, in which a thin beam of ions is extracted from a plasma ion source, focused and accelerated through a potential of tens to hundreds of kilovolts, and delivered to the target material. Then the beam and target are manipulated to expose the target surface to the beam until the desired dose is accumulated. Some drawbacks of conventional implantation are ion source and beam scanning complexity and maintenance, low beam current, nonuniform implantation profile, and low energy efficiency per implanted ion.

In plasma immersion ion implantation (PIII), the intermediate stages of ion source, beam extraction, focusing and scanning are omitted. The target is immersed in a plasma environment, and ions are extracted directly from the plasma and accelerated into the target by means of a series of negative, high voltage pulses applied to the target. Both metallurgical[1–5] and semiconductor[6] implantation processes have been demonstrated using PIII.

When a sudden negative voltage is applied to the target, then, initially, on the timescale of the inverse electron plasma frequency ω_{pe}^{-1}, electrons near the surface are driven away, leaving behind a uniform density ion "matrix" sheath. Subsequently, on the timescale of the inverse ion plasma frequency, ions within the sheath are accelerated into the target. This, in turn, drives the sheath-plasma edge further away, exposing new ions that are extracted. On a longer timescale, the system evolves toward a steady state Child law[7] sheath. Generally, this is of no interest in PIII, because the sheath thickness exceeds the plasma size; hence the voltage is returned to zero before the steady state sheath forms.

The matrix sheath and its time evolution determine the current $J(t)$ and the energy distribution dN/dW of implanted ions. The structure of the initial matrix sheath in one-dimensional planar, cylindrical, and spherical targets[8] and two-dimensional wedge-shaped targets[9] has been determined. In addition, the self-consistent equations have been solved numerically to find the time evolution of the matrix sheath in planar geometry[10-11]. However, it is desirable to have an analytical estimate of J and dN/dW. In this study, we develop an approximate analytical model for an applied rectangular voltage pulse in one-dimensional planar geometry and compare the results with the numerical solutions. The model yields quantities, such as the peak implantation current and time, and their scalings with system parameters, that are useful in describing the PIII process.

II. BASIC MODEL

Figure 1a shows the initial PIII geometry. The planar target is immersed in a uniform plasma of density n_0. At time $t = 0$, a voltage pulse of amplitude $-V_0$ and time width t_p is applied to the target, and the plasma electrons are driven away to form the matrix sheath, with sheath edge at $x = s_0$. As time evolves (Fig. 1b), ions are implanted, the sheath edge recedes, and a nonuniform, time-varying sheath forms near the target. The model assumptions are:

(1) The ion flow is collisionless. This is valid for sufficiently low gas pressures.

(2) The electron motion is inertialess. This follows because the characteristic implantation timescale much exceeds ω_{pe}^{-1}.

(3) The applied voltage V_0 is much greater than the electron temperature T_e; hence the Debye length $\lambda_D \ll s_0$, and the sheath edge at s is abrupt.

(4) During and after matrix sheath implantation, a quasistatic Child law sheath forms. The current demanded by this sheath is supplied by the uncovering of ions at the moving sheath edge and by the drift of ions toward the target at the Bohm (ion sound) speed $u_B = (eT_e/M)^{1/2}$.

(5) During the motion of an ion across the sheath, the electric field is frozen at its initial value, independent of time, except for the change in field due to the velocity of the moving sheath.

Assumptions (4) and (5) are approximations that permit an analytical solution to the sheath motion. These assumptions are justified *post hoc* by comparison with numerical results.

III. SHEATH MOTION

The Child law current density j_c for a voltage V_0 across a sheath of thickness s is[7]

$$j_c = \frac{4}{9}\varepsilon_0 \left[\frac{2e}{M}\right]^{1/2} \frac{V_0^{3/2}}{s^2} , \tag{1}$$

where ε_0 is the free space permittivity and e and M are the ion charge and mass. Equating j_c to the charge per unit time crossing the sheath boundary,

$$en_0(\frac{ds}{dt} + u_B) = j_c , \tag{2}$$

we find the sheath velocity

$$\frac{ds}{dt} = \frac{2}{9}\frac{s_0^2 u_0}{s^2} - u_B , \tag{3}$$

where

$$s_0 = \left[\frac{2\varepsilon_0 V_0}{en_0}\right]^{1/2} \tag{4}$$

is the matrix sheath thickness and

$$u_0 = (2eV_0/M)^{1/2} \tag{5}$$

is the characteristic ion velocity. Integrating (3), we obtain

$$\tanh^{-1}(s/s_c) - s/s_c = u_B t/s_c + \tanh^{-1}(s_0/s_c) - s_0/s_c , \tag{6}$$

where

$$s_c = s_0 \left[\frac{2}{9}\frac{u_0}{u_B}\right]^{1/2} \tag{7}$$

is the steady state Child law sheath thickness. Since $s_c \gg s_0$ and assuming $s_c \gg s$, we obtain from (6) that

$$\frac{s^3}{s_0^3} = \frac{2}{3}\omega_{pi}t + 1 , \tag{8}$$

where $\omega_{pi} = u_0/s_0$ is the ion plasma frequency in the matrix sheath. Substituting (7) into (8), we note that the timescale t_c for establishing the steady state Child law sheath is $t_c \approx (4/9)\,\omega_{pi}^{-1}(V_0/T_e)^{3/2}$, and we assume that the pulse width $t_p \ll t_c$ in the development that follows.

IV. MATRIX SHEATH IMPLANTATION

Because the initial charge density in the matrix sheath is uniform, the initial electric field varies linearly with x: $E = \omega_{pi}^2(x - s)$. Hence, the ion motion is

$$\frac{d^2x}{dt^2} = \omega_{pi}^2(x - s)\ . \tag{9}$$

Approximating $s = s_0 + (ds/dt)_0 t$ in (9) and using (3) with $s = s_0$ and $u_B \ll u_0$, we obtain

$$\frac{d^2x}{dt^2} = \omega_{pi}^2(x - s_0) - \frac{2}{9}u_0\omega_{pi}^2 t\ . \tag{10}$$

Integrating (10), we find

$$x - s_0 = (x_0 - s_0)\cosh\omega_{pi}t - \frac{2}{9}s_0\sinh\omega_{pi}t + \frac{2}{9}u_0 t\ , \tag{11}$$

where we have let $x = x_0$ and $\dot{x} = 0$ at $t = 0$. Letting $x = 0$ in (11), we obtain the ion flight time t from

$$s_0 = (s_0 - x_0)\cosh\omega_{pi}t + \frac{2}{9}s_0\sinh\omega_{pi}t - \frac{2}{9}u_0 t\ . \tag{12}$$

In a time interval between t and $t+dt$, ions from the interval between x_0 and x_0+dx_0 are implanted. Differentiating (12), we find

$$\frac{dx_0}{dt} = \frac{\omega_{pi}(s_0-x_0)\sinh\omega_{pi}t + \frac{2}{9}u_0(\cosh\omega_{pi}t - 1)}{\cosh\omega_{pi}t}\ . \tag{13}$$

Using (12) in (13) to eliminate s_0-x_0, we obtain the implantation current density $j = en_0\,dx_0/dt$ as

$$J = \frac{\sinh T}{\cosh^2 T} + \frac{2}{9}\,\frac{1 + T\sinh T - \cosh T}{\cosh^2 T}\ , \tag{14}$$

where $J = j/(en_0u_0)$ is the normalized current density and $T = \omega_{pi}t$ is the normalized time. Equation (14) gives the implantation current density versus time for those ions in the initial matrix sheath $0 \le x_0 \le s_0$. Setting $x_0 = s_0$ in (12), we obtain $T \approx 2.7$. At this time, all matrix sheath ions are implanted; hence (14) is valid for $0 \le T \le 2.7$. Figure 2 gives a plot of J versus T. The maximum

$J_{\max} \approx 0.55$ occurs at $T_{\max} \approx 0.95$. We note that $J(2.7) \approx 0.19$.

V. QUASISTATIC CHILD LAW SHEATH IMPLANTATION

Consider the implanted ions having initial positions at $x_0 > s_0$. The time t_s for the initial sheath edge at s_0 to reach x_0 is found from (8):

$$\omega_{pi} t_s = \frac{3}{2}\frac{x_0^3}{s_0^3} - \frac{3}{2} . \tag{15}$$

At time t_s, an ion at x_0 begins its flight across the sheath. The ion flight time is given by[7]

$$\omega_{pi} t' = 3 x_0 / s_0 . \tag{16}$$

Hence, an ion at x_0 reaches the target at a time $t = t_s + t'$ given by

$$T = \omega_{pi} t = \frac{3}{2}\frac{x_0^3}{s_0^3} - \frac{3}{2} + 3\frac{x_0}{s_0} . \tag{17}$$

Differentiating (17), we obtain

$$\frac{dx_0}{dt} = \frac{u_0}{\frac{9}{2}\frac{x_0^2}{s_0^2} + 3} . \tag{18}$$

The normalized implantation current density is thus

$$J = \frac{1}{\frac{9}{2}\frac{x_0^2}{s_0^2} + 3} . \tag{19}$$

Equations (17) and (19) give $J(T)$ as a parametric function of x_0/s_0 (Although (17) can be solved for x_0 and substituted into (18), the result is not illuminating). For $x_0/s_0 = 1$, we find $T = 3$ and $J(3) = 2/15 \approx 0.133$. As $T \to \infty$, $x_0 \to s_c \gg s_0$; hence $J(\infty) \to (2/9) s_0^2/s_c^2$. Unnormalizing, we find $j(\infty) \to e n_0 u_B$, which correctly gives the steady state Child law current density. However, as noted previously, we are not interested in this long timescale.

We note that (14) and (19) do not smoothly join at $x_0 = s_0$. This is a consequence of the simplifying assumptions (4) and (5) that were used to solve for the sheath and ion motion. Figure 2 shows the analytical results for J versus T in both regimes.

The nonlinear partial differential equations for the ion and electron motion in the planar sheath have been solved numerically by Conrad[10–11]. The ion motion is collisionless, the electrons are in thermal equilibrium, and Poisson's equation relates the densities to the potential. The equations are:

$$\frac{\partial n_i}{\partial t} + \frac{\partial}{\partial x}(n_i u_i) = 0 ,$$

$$M\frac{\partial u_i}{\partial t} + M u_i \frac{\partial u_i}{\partial x} = -e\frac{\partial \Phi}{\partial x} ,$$

$$n_e = n_0 \exp(-\Phi/T_e) ,$$

$$\frac{\partial^2 \Phi}{\partial x^2} = -\frac{e}{\varepsilon_0}(n_i - n_e) .$$

Figure 2 shows a numerical solution for $V_0/T_e = 200$. We see that (14) for $T < 2.7$ and (19) for $T > 3$ are in good agreement with the numerical results. A numerical solution for $V_0/T_e = 50$ also agrees well with the analytical model, and the predicted scaling $j \propto V_0^{1/2}$ is verified numerically.

VI. ENERGY DISTRIBUTION

We assume a voltage pulse of width $T > 3$, such that all matrix sheath ions ($x_0 \le s_0$) are implanted. For these ions, since the potential varies quadratically with the distance from the sheath edge, ions starting at x_0 are implanted with energy

$$W = V_0\left[1 - \frac{(s_0 - x_0)^2}{s_0^2}\right] . \tag{20}$$

Within the energy interval $dW = 2V_0(s_0 - x_0)\,dx_0/s_0^2$, there are $dN = n_0 dx_0$ ions per unit area implanted. Hence, we find

$$\frac{dN}{dW} = \frac{n_0 s_0^2}{2} V_0 (s_0 - x_0) . \tag{21}$$

Using (20) in (21), we find the energy distribution for the matrix ions:

$$\frac{dN}{dW} = \frac{n_0 s_0}{2 V_0^{1/2}}(V_0 - W)^{-1/2} . \tag{22}$$

For a pulse of width $T > 3$, all ions from the interval $s_0 \le x_0 \le x_T$ are implanted at full energy, where x_T is determined from (17):

$$\frac{3}{2}\frac{x_T^3}{s_0^3} - \frac{3}{2} + 3\frac{x_T}{s_0} = T \ . \tag{23}$$

Hence, the energy distribution contains a delta function, $dN/dW = n_0(x_T - s_0)\,\delta(W - V_0)$, for these ions.

Finally, because the sheath edge s_T has reached the position given by (15),

$$\frac{3}{2}\frac{s_T^3}{s_0^3} - \frac{3}{2} = T \ , \tag{24}$$

all ions with $x_T \le x_0 \le s_T$ are in transit when the pulse is turned off. The density and potential in the Child law sheath just before turnoff are[7]

$$n(x) \propto \left[\frac{s_T}{s_T - x}\right]^{1/3} \tag{25}$$

and

$$\Phi(x) = V_0\left[\frac{s_T - x}{s_T}\right]^{5/3} . \tag{26}$$

Using (26), the ion energy is

$$W(x) = V_0\left[1 - \left[\frac{s_T - x}{s_T}\right]^{5/3}\right] . \tag{27}$$

Differentiating (27) to obtain dW and using $dN = n(x)\,dx$, we find

$$\frac{dN}{dW} \propto \frac{s_T}{s_T - x} \ . \tag{28}$$

Using (27) in (28) and normalizing the distribution such that $N = n_0(s_T - x_T)$, we obtain

$$\frac{dN}{dW} = \frac{2}{5}\frac{(s_T - x_T)n_0}{V_0^{2/5}}(V_0 - W)^{-3/5} . \tag{29}$$

The total energy distribution is the sum of the distributions for ions having $0 \le x_0 \le s_0$, $s_0 \le x_0 \le x_T$ and $x_T \le x_0 \le s_T$. The total dose implanted is $n_0 s_T$.

A quantity of interest is the fraction f of ions that hit the target with $W < W_{\min} < V_0$. For example, ions with energies below several kilovolts may produce sputtering of the target rather than be implanted. Integrating (22) and (29) from 0 to $W_{\min}$, we obtain

$$f = \frac{s_0}{s_T}\left[1 - \left(1 - \frac{W_{\min}}{V_0}\right)^{1/2}\right] + \left(1 - \frac{x_T}{s_T}\right)\left[1 - \left(1 - \frac{W_{\min}}{V_0}\right)^{2/5}\right] . \qquad (30)$$

Figure 3 shows f versus T for various values of $W_{\min}/V_0$.

ACKNOWLEDGMENT

This work was supported by a contract from IBM Corporation, a grant from Applied Materials Corporation, National Science Foundation Grant ECS-8517363, and Department of Energy Grant DE-FG03-87ER13727. Helpful discussions with I. Brown, D.A. Carl, N.W. Cheung, H. Wong, X. Qian, and S.E. Savas are gratefully acknowledged.

REFERENCES

1. J.R. Conrad and C. Forest, in *IEEE International Conference on Plasma Science*, Saskatoon, Canada, May 19-21, 1986 (IEEE, New York).
2. J.R. Conrad and T. Castagna, *Bull. Am. Phys. Soc.* 31, 1479 (1986).
3. J.R. Conrad, J.L. Radtke, R.A. Dodd, F.J. Worzala, and N.C. Tran, *J. Appl. Phys.* 62, 4591 (1987).
4. J.R. Conrad, S. Baumann, R. Fleming and G.P. Meeker, *J. Appl. Phys.* 65, 1707 (1989).
5. J. Tendys, I.J. Donnelly, M.J. Kenny and J.T.A. Pollack, submitted to *Appl. Phys. Lett.* (1988).
6. H. Wong, X. Quian, D. Carl, N.W. Cheung, M.A. Lieberman, I. Brown, and K.M. Yu, submitted to *Applied Physics Letters*, 1989.
7. C.D. Child, *Phys. Rev.* 32, 492 (1911).
8. J.R. Conrad, *J. Appl. Phys.* 62, 777 (1987).
9. I.J. Donnelly and P.A. Watterson, *J. Phys. D: Appl. Phys.* 22, 90 (1989).
10. J.R. Conrad, "Plasma Source Ion Implantation", presented at United Technologies Research Center, Sept. 26, 1986 (unpublished).
11. J.R. Conrad and T. Castagna, in *Proceedings of the 39th Annual Gaseous Electronics Conference*, Madison, WI, October 7-10, 1986.

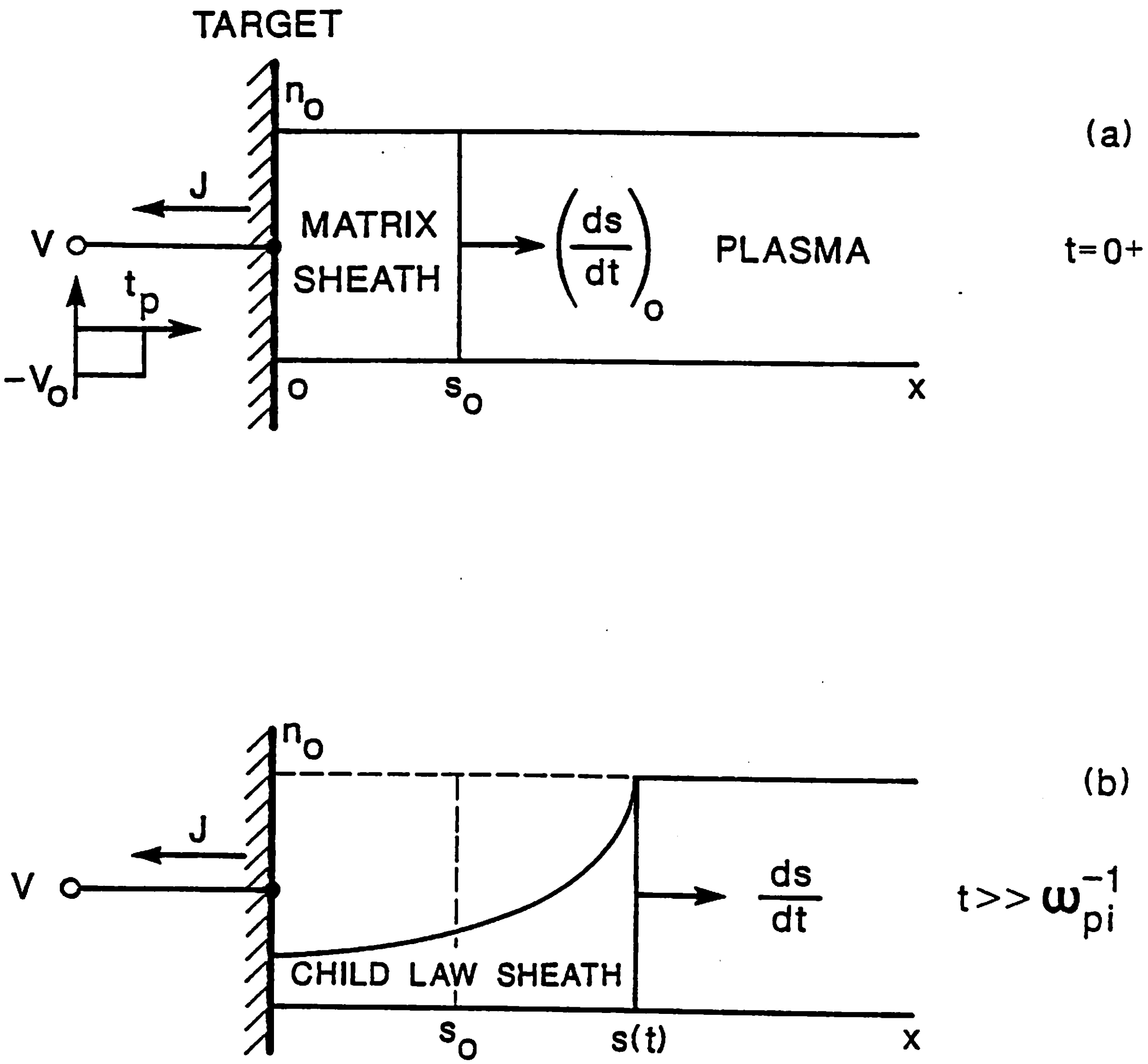

Fig. 1. Planar PIII geometry (a) just after formation of the matrix sheath and (b) after evolution of the quasistatic Child law sheath.

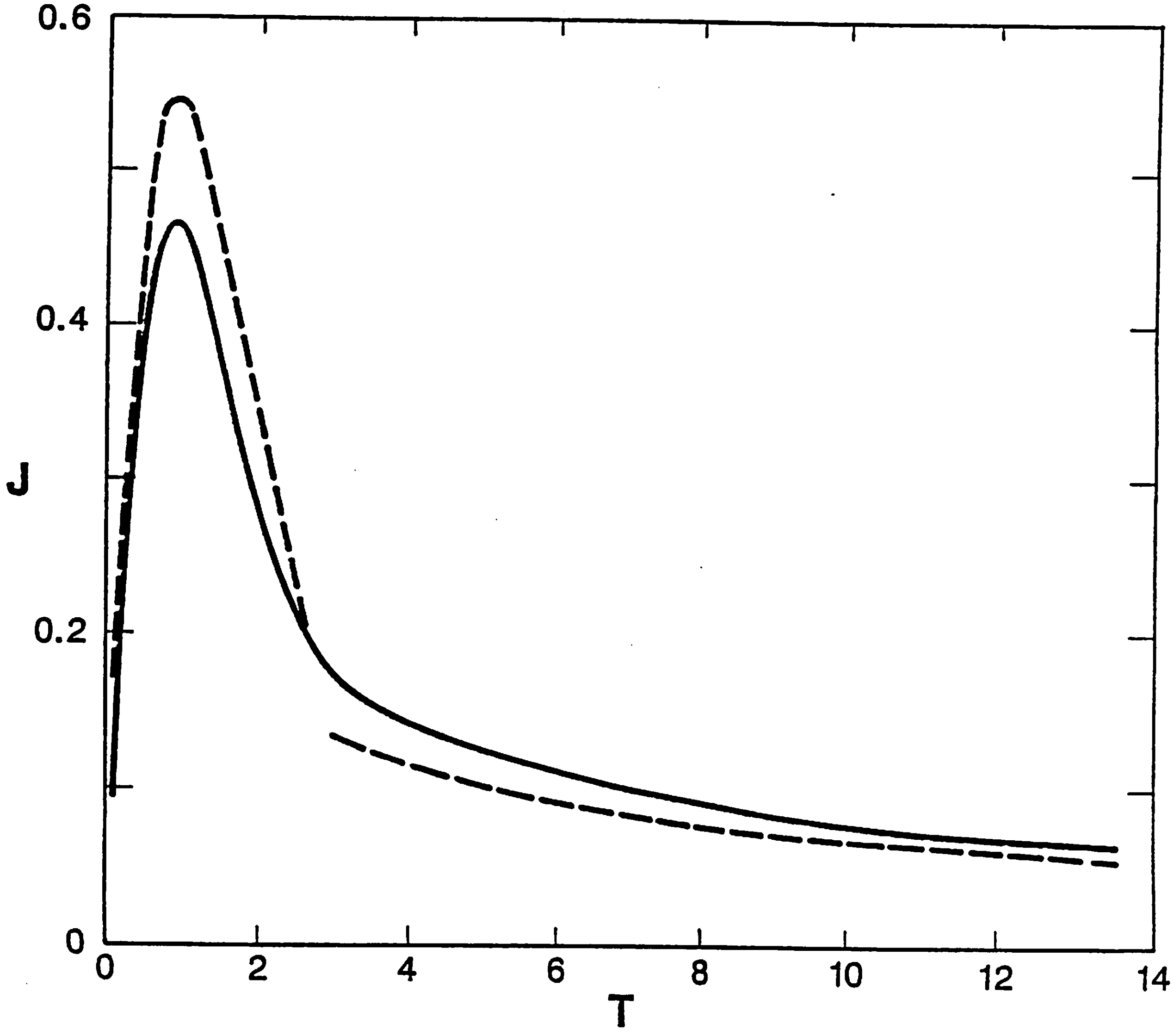

Fig. 2. Normalized implantation current density $J = j/(en_0u_0)$ versus normalized time $T = \omega_{pi}t$. The dashed lines show the analytical solution for $T < 2.7$ [Eq. (14)] and $T > 3$ [Eq. (19)]; the solid line is the numerical solution of Conrad[10].

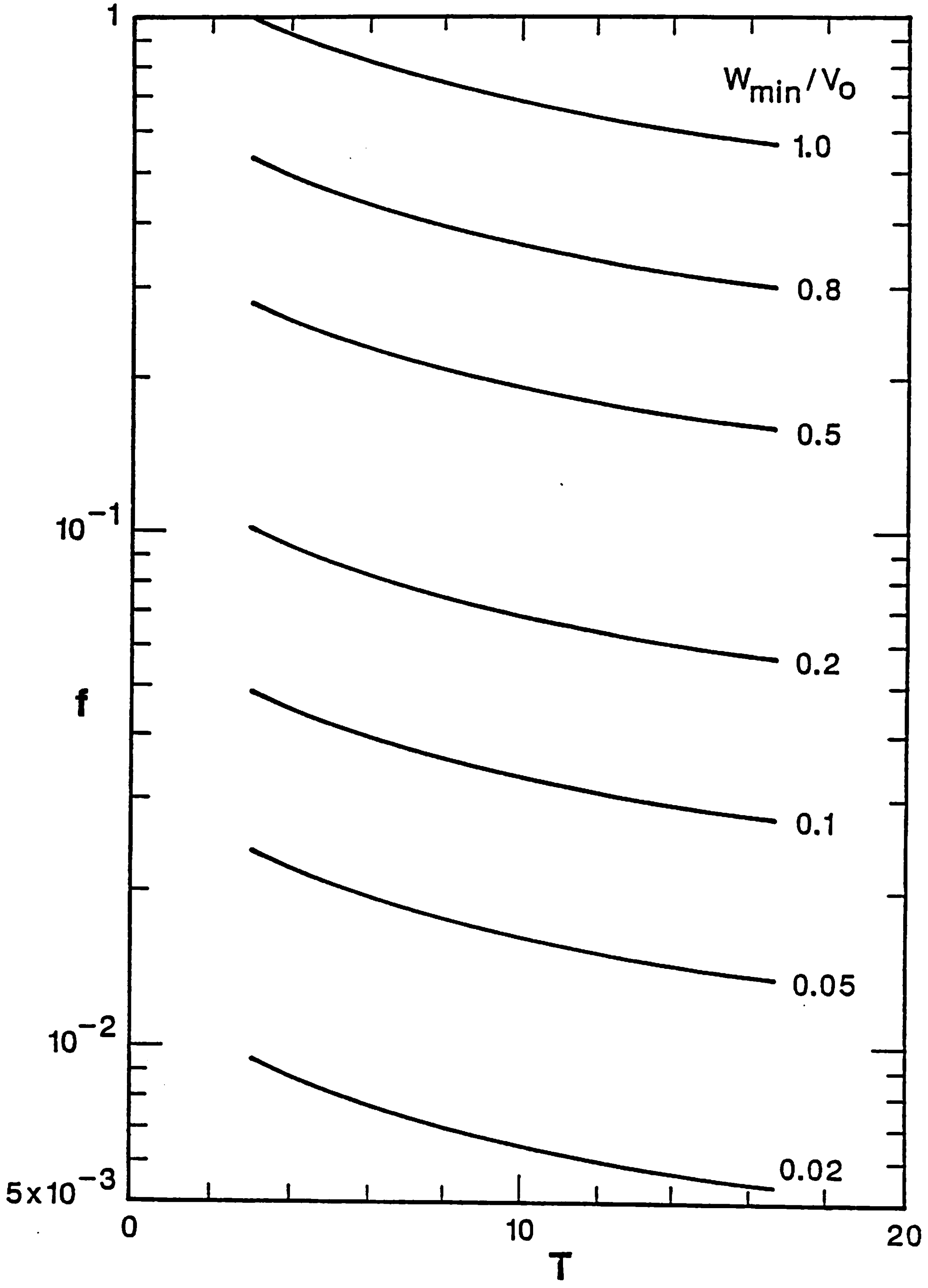

Fig. 3. Fraction f of ions hitting the target with energies $W < W_{\min}$ versus T, with $W_{\min}/V_0$ as a parameter.